Journal of Mining and Environment (JME) Vol. 18, No. 4, 2026, 1195-1213

Shahrood University of Technology

Journal of Mining and Environment (JME)

Journal homepage: www.jme.shahroodut.ac.ir

Iranian Society of Mining Engineering (IRSME)

Structural Control of Cobalt Mineralization in the Aït Ahmane Region – Bou Azzer El Grara Inlier (Central Anti-Atlas, Morocco): Contribution of remote sensing and underground geological mapping

Abdelhamid Bajadi[1], Driss El Azzab[1], Anas Driouch[2], Mohammed Ouchchen[3], and Mohammed Jalal Tazi[1*]

1. Science and Engineering Research Laboratory (LaRSI), Faculty of Sciences and Technology, Sidi Mohamed Ben Abdellah University, Fez, Morocco
2. Laboratory of Applied Geophysics, Geotechnics, Engineering Geology and the Environment, Mohammadia School of Engineers, Mohammed V University, Rabat, Morocco
3. Department of Earth Sciences, Faculty of Sciences, Ibn Zohr University, Agadir, Morocco

Article Info

Received 16 September 2025

Received in Revised form 31 December 2025

Accepted 10 May 2026

Published online 10 May 2026

DOI: 10.22044/jme.2026.16825.3302

Keywords

Underground geological mapping

Structural control

Cobalt

Mineral exploration

Bou Azzer El Grara inlier

Abstract

The Bou Azzer–El Graara inlier, located in Morocco's central Anti-Atlas, is well known for its significant cobalt mineralization, genetically associated with a Pan-African serpentinized ultrabasic ophiolitic massif. In this context, a structural study was conducted in the Aït Ahmane area, situated at the eastern end of the Bou Azzer mining district, with the aim of analyzing structural lineaments, which constitute a fundamental tool in geological mapping and mineral exploration. The methodological approach is based on the interpretation of multispectral remote sensing data to map surface lineaments and compare them with structures observed underground. The processing applied to the Landsat 8 OLI imagery includes radiometric and atmospheric corrections, followed by principal component analysis (PCA), which enhances the discrimination of linear structures and allows the production of reliable lineament maps. In parallel, underground geological mapping was carried out in the F53 vein deposit, at two lower exploitation levels, to characterize mineralized structures at depth. The integration of surface and subsurface datasets highlights two main structural families. The first, trending N–S to NE–SW, is associated with cobalt-bearing structures hosted within diorites. The second, oriented NW–SE to WNW–ESE, corresponds to cobalt-mineralized tectono-lithological contacts between serpentinites, basic rocks, and diorites. The correlation between surface-mapped lineaments and deep-seated structures is significant, emphasizing the structural continuity between the surface and subsurface domains.

1. Introduction

The critical metals, particularly cobalt, play a pivotal role in the global energy transition and in efforts to mitigate climate change. Primarily used in the manufacture of lithium-ion batteries for electric vehicles and renewable energy storage systems, cobalt has become a strategic material at the center of major international geopolitical and industrial concerns [1–3]. In this context, efforts to strengthen the primary cobalt supply chain must be addressed in an integrated manner across the entire mining life cycle, from upstream stages of prospecting and exploration to downstream phases of development and production. Coordinated optimization of these stages, encompassing responsible exploration, sustainable mine development, efficient production practices, and rigorous post-mining environmental

Corresponding author: mohammedjalaltazi.tazi@usmba.ac.ma (M.J. Tazi)

management is essential to ensure the traceability, sustainability, and security of cobalt supply. The present study is embedded within this comprehensive framework, with a specific focus on the upstream phase of the mining cycle. Its objective is to contribute to the identification and exploration of new cobalt resources in Morocco to meet the growing demand for this strategic material, while accounting for the geological, environmental, and socio-economic constraints inherent to the national context.

Among strategic exploration methods that have demonstrated strong effectiveness in mapping mineral-potential zones, remote sensing has gained increasing prominence. It enables rapid, large-scale identification of geological structures and polyphase tectonic settings that may control the localization of cobalt mineralization [4–6]. This indirect approach is particularly well suited to the investigation of extensive areas, especially in regions that are difficult to access and characterized by arid to semi-arid climatic conditions, where vegetation cover is sparse or absent. By providing a synoptic view of the terrain, remote sensing constitutes a key tool for guiding and optimizing early-stage mineral exploration. Remote sensing is based on the analysis of satellite imagery acquired by sensors such as ASTER, Sentinel, and Landsat. Among these systems, Landsat 8 OLI (Operational Land Imager) imagery stands out for its effectiveness in geological mapping, owing to its 30-m spatial resolution and the configuration of its spectral bands, which are well suited for lithological discrimination and structural identification [7]. Multispectral analysis, particularly through techniques such as principal component analysis (PCA) and color composite generation, enhances spectral contrasts and enables the detection of structural lineaments and spectral anomalies that may be associated with mineralized zones. This approach is now widely applied in mineral exploration, especially in geologically complex and inaccessible environments where conventional field-based methods are constrained [7–9].

This study focuses on the Bou Azzer-El Graara inlier, located in the central part of the Anti-Atlas mountain range. The area is of major geological and geodynamic significance and is characterized by a high degree of lithological diversity, including strongly tectonized formations ranging in age from the Tonian to the Ediacaran, unconformably overlain by Paleozoic sedimentary deposits [10]. From an economic perspective, the inlier represents a key mining district, hosting the well-known Bou Azzer and Bleida mines [6]. Cobalt mineralization within the Bou Azzer district is closely controlled by two principal factors. The first is the presence of Neoproterozoic ophiolitic serpentinite massifs of ultrabasic composition [11–16]. The second relates to the region's complex tectonic evolution, which has generated numerous structures of varying ages and geological contexts, exerting a direct influence on the spatial distribution of mineral deposits. In this regard, a comprehensive understanding of the interactions between local lithology, regional geological setting, and successive tectonic events is essential for both structural interpretation and the optimization of exploration and mining strategies [17– 20]. Within this framework, an in-depth investigation was conducted in the Aït Ahmane area, which is currently the focus of major mining development projects involving several cobalt-bearing deposits. This area has been the subject of recent geological studies; for example, [21] investigated the F53 deposit, while [22] also concentrated their work on this site. In contrast, the present study extends the scope of analysis to the entire Aït Ahmane region, which hosts multiple mineralized zones beyond the F53 deposit alone. The semi-arid climate and sparse vegetation cover of the region prompted the adoption of a digital mapping approach based on remote sensing for lineament extraction [23,24]. Several pre-processing and image enhancement techniques were applied to improve data quality and interpretability. These analyses were complemented by detailed field investigations, including geological mapping aimed at identifying the main mineralized structures (faults and lithological contacts), as well as their orientations and deformation styles. Structural mapping of the Aït Ahmane area revealed widespread ophiolitic outcrops and a high concentration of cobalt mineralization. The deposits occur predominantly as vein-type mineralization within diorites, as well as in clusters localized along contacts between ophiolites, diorites, and diabase units [6,22,25]. Accordingly, the objectives of this study are twofold: (i) to characterize the structural controls on cobalt mineralization by correlating lineaments identified through remote sensing with field-based structural observations, and (ii) to contribute to ongoing national and international efforts aimed at advancing the exploration of strategic and critical metals.

2. Geology of the Study Area

2.1. Lithological context

The Bou Azzer–El Grara inlier is part of the Central Anti-Atlas and marks the Anti-Atlas Major Fault (AAMF) in a NW–SE direction [13] (Figure 1a, b). The Ait Ahmane study area is located in the eastern part of this inlier (Figures 1b and 2).

The exposed rocks in the study area belong to the Precambrian basement and comprise Tonian, Cryogenian, and Ediacaran terranes, unconformably overlain by a Paleozoic sedimentary cover.

The Upper Tonian to Lower Cryogenian terranes, forming the Tachdamt–Bleida Group, are composed mainly of siltstones, sandstone–quartzite successions, and basaltic units [27]. The Lower Cryogenian succession includes fine-grained siltstones assigned to the Tichibanine–Ben Lgrad Group, together with orthogneisses, metamorphosed mafic rocks, paragneisses, amphibolites, and metagabbros [15,28].

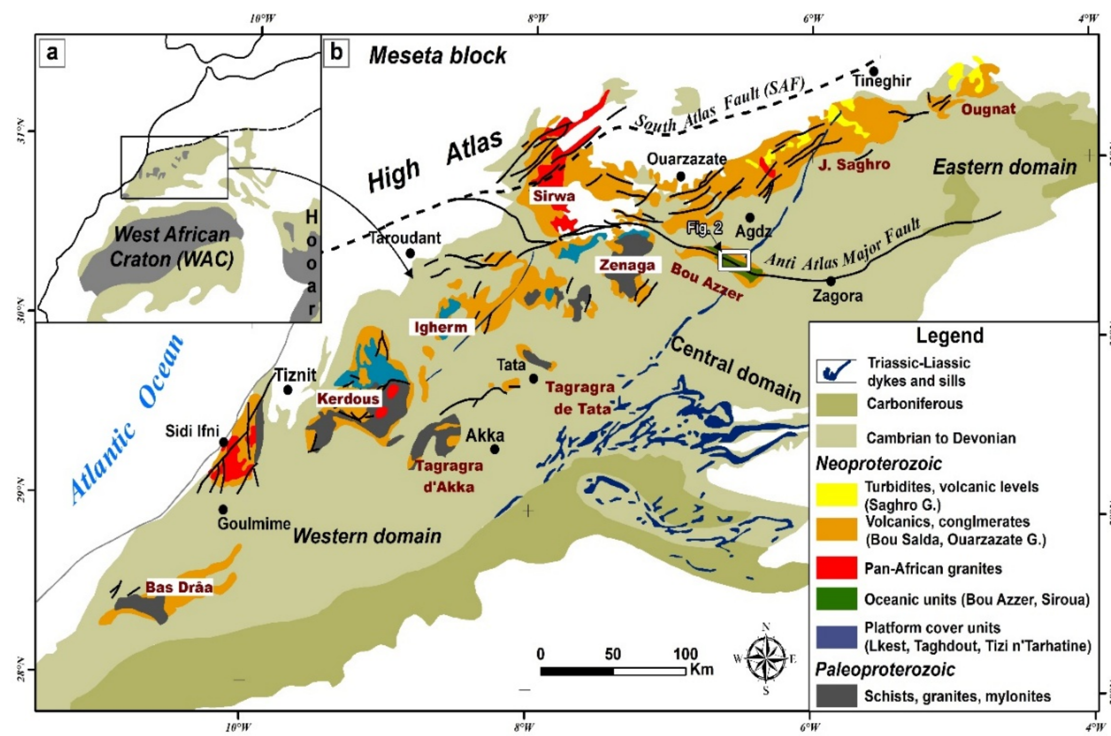

Figure 1. (a) The location of Moroccan anti – Atlas, (b) The general geological map of the anti-Atlas shows the location of the study area [26]

The Bou Azzer Group, corresponding to an Upper Cryogenian terrane, is represented by a well-developed ophiolitic complex consisting of serpentinized mantle peridotites, microgabbro–dolerite dykes, basalts, and associated volcano-sedimentary sequences [13,25,29]. This ophiolitic complex is intruded and locally overlain by the polyphase Taghouni massif, which is composed predominantly of dioritic and granodioritic intrusions [10]. Overlying these units, ignimbrites and andesites of the Lower Ediacaran Bou Lbarod–Iouraghene Group are present, followed by the Tiddiline Group, also of Lower Ediacaran age, which consists mainly of sandstones and siltstones. The Ouarzazate Group (Upper Ediacaran) is characterized by a volcano-clastic succession dominated by rhyolites, dacites, andesites, and tuffs [10,13,15,26]. The Precambrian basement is unconformably overlain by a thick Paleozoic (Infra-Cambrian) sedimentary cover, known as the Adoudounian, which comprises a succession of clastic and carbonate deposits [30,31].

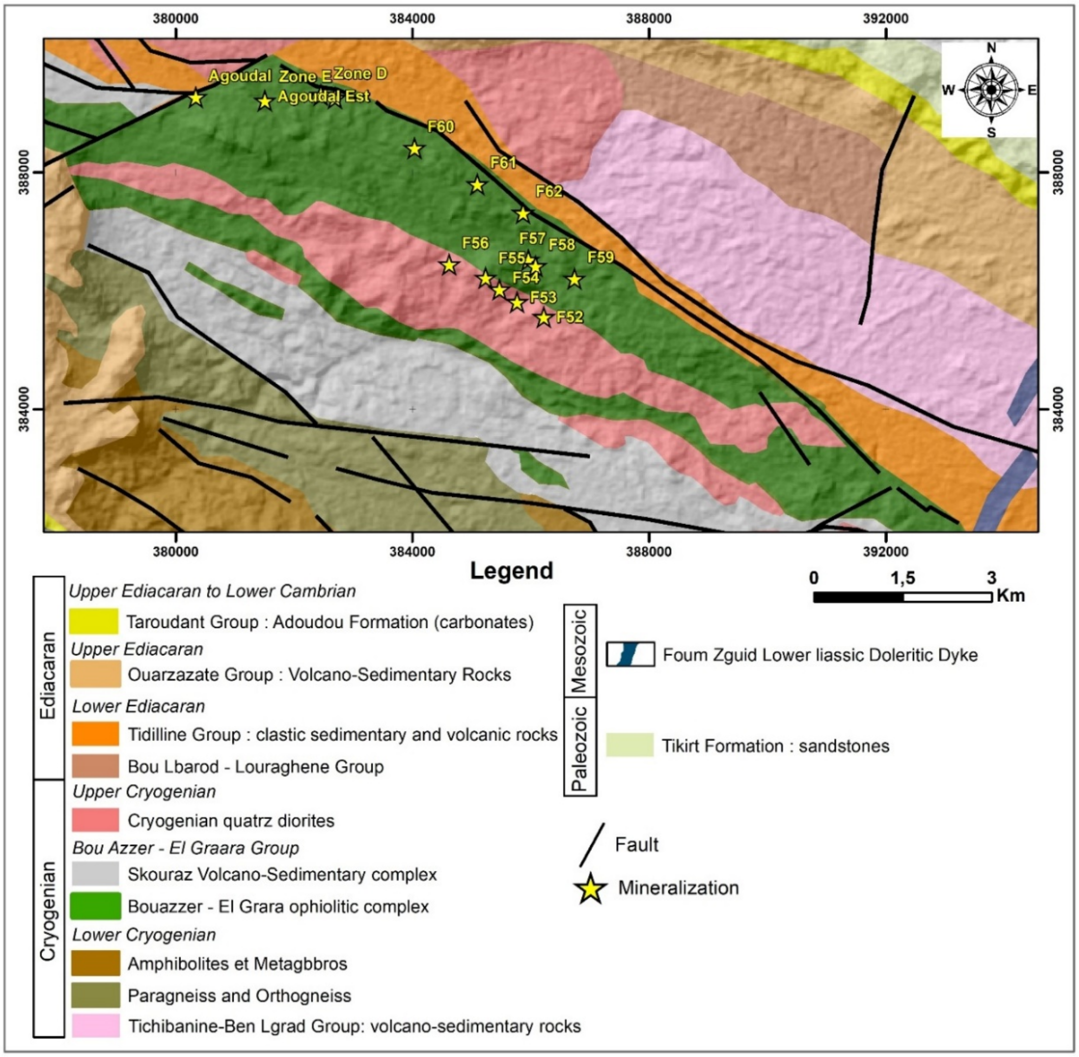

Figure 2. Geological map of the study area [15]

2.2. Structural context

The Bou Azzer–El Graara inlier is located along the Anti-Atlas Major Fault, which is interpreted as the Neoproterozoic Pan-African suture of the Anti-Atlas belt [28, 32– 35]. Its structure is dominated by a basal thrust surface related to the obduction of the Bou Azzer ophiolitic complex onto Cryogenian formations, which is presently folded into a recumbent anticline, reflecting intense Pan-African compressional deformation [11,36].

Structural analysis reveals a polyphase fault network organized into three main structural systems:

i. WNW–ESE to ONO–ESE faults, inherited from Pan-African tectonics and reactivated during the Hercynian orogeny, form the structural backbone of the inlier and control the main lithological contacts between serpentinites, ophiolitic gabbros, dioritic intrusions, and Ediacaran volcano-sedimentary formations [21,36,37].

ii. NW–SE dextral shear zones, interpreted as Pan-African C/S shear planes, record a transpressional regime and promoted ductile to ductile–brittle deformation as well as hydrothermal fluid circulation [28,36].

iii. Late N–S and NE–SW faults, attributed to the Hercynian orogeny, cut both the Proterozoic basement and the Lower Cambrian sedimentary cover. Among these structures, the Ightem fault is the most continuous and regionally extensive, affecting even the carbonates of the Adoudou Formation [15,21,36].

2.3. Gitology

The Co–Ni arsenide deposits of the Bou Azzer district are hosted within a structurally complex ore system controlled by the superposition of Pan-African ductile to ductile–brittle deformation and subsequent Hercynian brittle reactivation. This polyphase tectonic evolution generated a favorable structural architecture that governs the localization, geometry, and remobilization of cobalt mineralization [15,22,25,38,39].

Cobalt mineralization systematically develops along contacts between hydrated ultramafic rocks (serpentinites) and adjacent lithologies, particularly quartz diorites and, locally, Ediacaran volcano-sedimentary units of the Ouarzazate Group [25,40,41]. The close spatial association between mineralization and serpentinites strongly suggests a genetic relationship, whereby serpentinites acted as the primary source of Co and Ni, subsequently leached and concentrated by hydrothermal fluids circulating along fault zones and shear corridors [15,25].

Recent studies refined this genetic model by distinguishing two main mineralization styles within the Bou Azzer district [6]. The first corresponds to contact-related mineralization, developed at the interface between serpentinite, quartz diorite, and volcano-sedimentary rocks of the Ouarzazate Group. The second style consists of Co-enriched mineralized faults, cutting both serpentinite and quartz diorite, reflecting late-stage hydrothermal remobilization associated with brittle deformation.

Based on mine-scale structural and morphological criteria [42], further classified the exploited mineralization into two principal ore types :

i) Massive mineralization, preferentially oriented N120°E, occurs as lenses or pocket-shaped bodies and is dominated by Ni–Co arsenides

ii) Vein-type cobalt arsenide mineralization, oriented N–S to N070°, is hosted in silica- and carbonate-rich gangue and is systematically localized along tectono-lithological contacts between serpentinite, quartz diorite, and Precambrian volcanic rocks.

Overall, the ore-deposit framework of the Bou Azzer district reflects a structurally controlled hydrothermal system, in which serpentinites played a dual role as both a metal source and a reactive host, while Pan-African deformation and Hercynian reactivation, controlled fluid pathways and ore emplacement.

3. Materials and methods

The study area is characterized by an arid climate, sparse vegetation cover, and limited cloud interference, conditions that are particularly favorable for the application of remote sensing techniques. In this context, a digital mapping approach based on satellite remote sensing was adopted to extract geological lineaments from Landsat 8 OLI imagery, which provides seven multispectral bands with a spatial resolution of 30 m.

Image pre-processing and analysis were conducted through several successive stages using ENVI image processing software. These stages included radiometric calibration and atmospheric correction using the QUAC algorithm, following established procedures [43]. To enhance spectral information and improve the discrimination of geological features, principal component analysis (PCA) was applied. This technique is widely recognized for its effectiveness in geological mapping using remote sensing data [44–50].

Lineament extraction was subsequently performed using the LINE module of Geomatica software. Multiple combinations of extraction parameters were tested to optimize the detection of linear features, in accordance with methodologies reported in previous studies [51–53]. The resulting lineament map was then carefully refined through visual interpretation and filtering to eliminate non-geological linear features, such as roads, drainage networks, and other anthropogenic or geomorphological elements.

To strengthen and validate the results derived from remote sensing, the methodological framework was complemented by detailed underground geological mapping conducted at the currently active mining site within the study area (F53). This approach enabled direct observation of structural features and their host lithologies at depth, thereby providing critical constraints for the interpretation of surface-derived lineaments. In parallel, synthetic geological cross-sections were constructed to support and refine the proposed structural interpretations.

Further validation was achieved through the application of the CET (Centre for Exploration Targeting) method to helicopter-borne magnetic data, with the objective of independently mapping structural lineaments. Detailed information regarding the characteristics of these magnetic data and their acquisition parameters is available in [54], entitled “Targeting potential cobalt deposits through integration of helicopter-borne magnetic and stream sediment data: Insights from the Bou Azzer Inlier, Central Anti-Atlas, Morocco”, to which the reader is referred for additional details. The CET method is widely recognized as an effective tool for geophysical exploration and structural mapping, particularly well suited for revealing complex geological structures and major linear trends that are critical for mineral exploration [55]. It relies on an automated lineament detection workflow comprising three main steps. First, a texture analysis is applied to the magnetic data to enhance local variations in the magnetic field and improve the detection of subtle structural features, thereby increasing the contrast associated with structural discontinuities. Second, a dedicated texture ridge detection technique is employed to identify lineaments exhibiting bilateral symmetry, derived from the texture analysis [56].

Finally, the detected texture ridges are refined through a thinning process, allowing the vectorization of linear segments and facilitating their integration into larger-scale geological and structural models. First, a texture analysis is applied to the magnetic data in order to enhance local variations in the magnetic field and improve the detection of subtle structural features. This step increases the contrast associated with structural discontinuities. Second, a dedicated texture ridge detection technique is implemented to identify lineaments exhibiting bilateral symmetry, derived from the texture analysis [56]. Finally, the detected texture ridges are refined through a thinning process, allowing the vectorization of linear segments and facilitating their integration into larger-scale geological and structural models.

Finally, an extensive review of the existing geological literature was conducted in order to place the results within their regional tectonic framework and to further refine the structural analysis. The integrated methodology combining satellite image processing, underground geological observations, validation through synthetic geological cross-sections, and magnetic data analysis is summarized in Figure 3, which highlights the structural complexity and the tectono-metallogenic context of the study area.

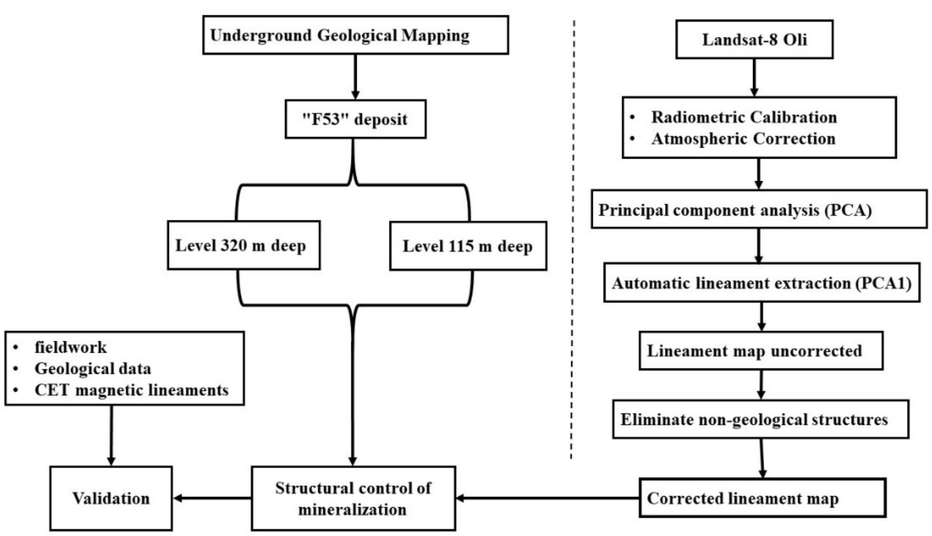

Figure 3. Methodology adopted for the study

4. Results and discussion

In this section, we present the main outcomes of this study, including the maps generated from the processing of Landsat satellite imagery, as well as the results of geological investigations carried out in the underground levels of the study area.

4.1. Landsat 8 Oli imagery

Regarding the results derived from satellite data processing, principal component analysis (PCA) was applied to the seven spectral bands (Bands 1–7) of the Landsat imagery. The first principal component (PC1), which captures the majority of the spectral information, was selected, accounting for 89.46% of the total variance (Table 1).

Based on PC1, a lineament map was generated following the methodology described above, along with a corresponding lineament density map. The latter highlights zones of high structural density, which are interpreted as areas of increased structural complexity and are therefore considered favorable sites for significant cobalt mineralization within the study area.

Table 1. Information content of each principal component

Main components	Variance	Information (%)
1	303,36	89,46
2	23,07	6,80
3	6,40	1,89
4	4,36	1,29
5	1,80	0,53
6	0,10	0,03
7	0,03	0,01
Total	339,1	100

4.1.1. Correction of the lineament map

The superimposition and compilation of the lineament maps derived from the first principal component (PC1) enabled the construction of a synthetic lineament map covering the entire study area. This map was subsequently refined through a correction process designed to improve data reliability and spatial accuracy. This process involved the removal of non-geological linear features, such as roads, rivers, built-up areas, and ridgelines, as well as the correction of geometric inconsistencies.

The resulting lineament map was validated using a two-step approach. First, a visual inspection was conducted using high-resolution satellite imagery available from Google Earth. Second, the extracted lineaments were compared with existing geological maps and field observations acquired during ground verification campaigns. This validation procedure ensured the geological relevance and robustness of the final lineament dataset.

4.1.2. Corrected map of lineaments

The results of the data processing yielded a corrected lineament map (Figure 4a) that reveals two main structural families: one oriented NE–SW and another displaying a dominant NW–SE to WNW–ESE trend. These structural features allow for the precise delineation of the various geological units and their boundaries.

The directional rose diagram of the extracted lineaments highlights a predominant NW–SE to WNW–ESE orientation, which closely corresponds to the contacts between the serpentinized ophiolitic complex and the surrounding host rocks, such as quartz diorites and gabbroic mafic units [41]. This structural trend not only reflects the inherent geological organization of the formations but also suggests active tectonic processes related to the reactivation of major contacts and regional fault systems. These aspects will be discussed in greater detail in the following sections.

In particular, these structural orientations are likely associated with movements along the Anti-Atlas Fault, a major tectonic structure that exerts a strong influence on both local and regional geodynamics. The NE–SW-oriented linear features are interpreted as reflecting extensional to transtensional tectonic structures within the Bou Azzer–El Grara inlier, and more specifically within the study area [57]. Lineament density, defined as the number of lineaments per unit area [58], constitutes a meaningful indicator for identifying zones of high structural concentration, which are commonly associated with intense tectonic deformation and enhanced mineral potential. In this study, a lineament density map was produced, revealing high concentrations of lineaments in the southern and northeastern parts of the study area, in contrast to the northern and northwestern sectors, where lineament density is comparatively lower (Figure 4b). This spatial distribution delineates structurally favorable zones that are likely to promote enhanced circulation of hydrothermal fluids and, consequently, the development of cobalt-bearing mineralization.

4.2. Geological and mining data

To complement the mapping of tectonic structures and to improve the understanding of the structural controls on cobalt mineralization in the Aït Ahmane region, detailed geological investigations were conducted, as described in the methodology, within the active underground workings of the study area. Accordingly, direct observations were carried out inside the galleries of the F53 mine, which represents the principal active site for analyzing structures associated with mineralization.

4.2.1. Geological mapping underground at a depth of 115 meters (-115)

The exploitation of cobalt-bearing mineralization at the F53 deposit is carried out across several underground levels, including the −115 level, which currently represents the main focus of both exploration and mining activities (Figure 5a).

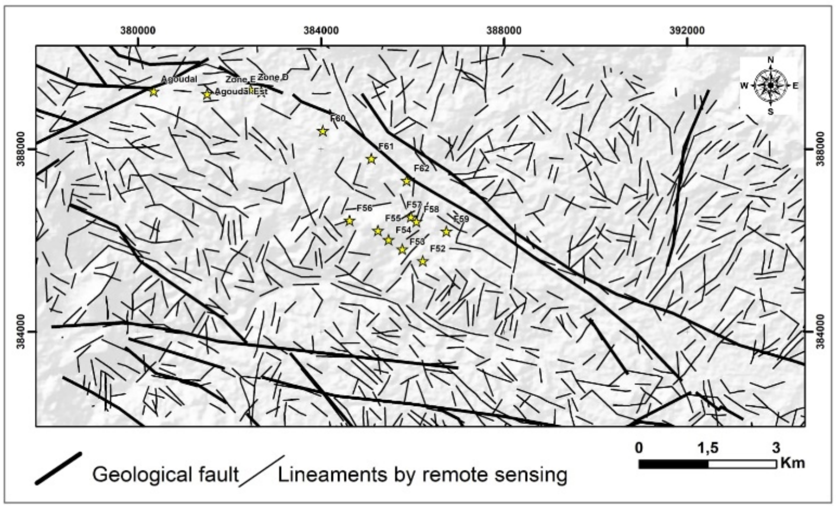

(a)

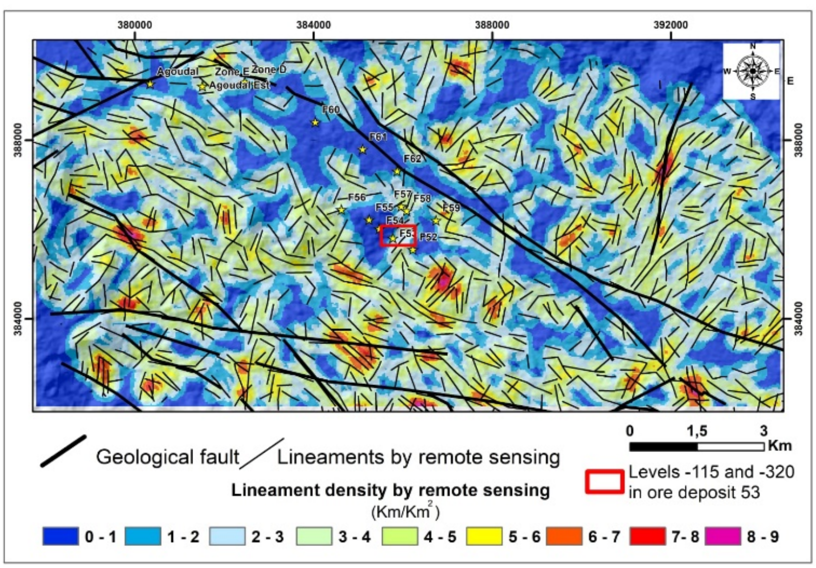

(b)

Figure 4. (a) Synthetic lineament map with corresponding directional rose diagram; (b) lineament density map

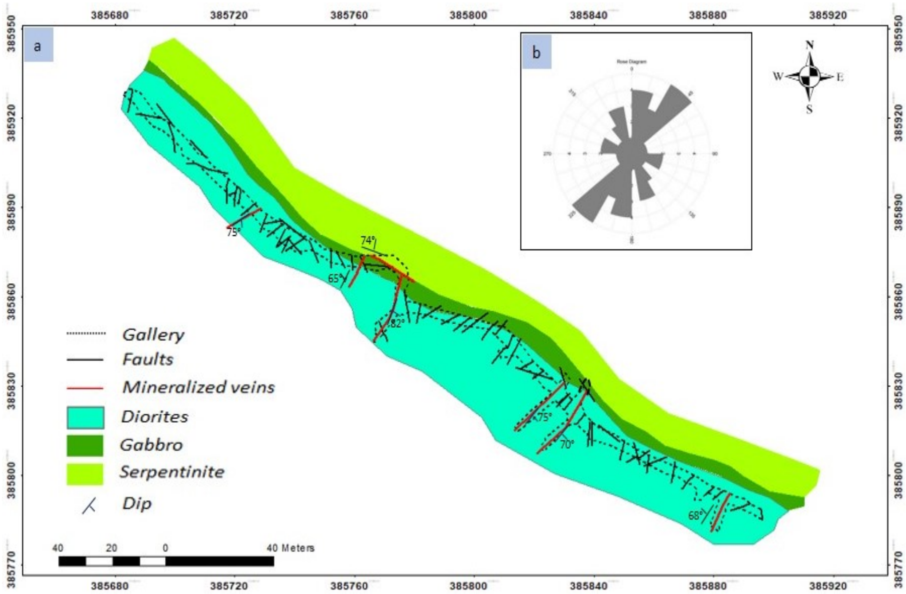

Figure 5. (a) Geological mapping of underground level –115; (b) Rose diagram of lineament orientations

The geological and structural survey conducted at this level reveals a gallery intersecting, on one hand, a complex fault system dominated by quartz–carbonate structures, and on the other hand, mineralized zones containing cobalt arsenides. A representative example is observed at the eastern end of the N–S-oriented gallery, where a structure filled with quartz–carbonate material contains traces of cobalt occurring as small veinlets.

Serpentinites are intersected only in sections of the gallery where they are in contact with bands of gabbroic (mafic) rocks. This ophiolitic unit displays a NW–SE orientation and dips approximately 75° to the north. Dioritic rocks, also intersected by the gallery, exhibit a granular texture with intense epidotization, indicating significant hydrothermal fluid circulation. The mineralized structures mapped at this level show orientations ranging between N10° and N15°, corresponding respectively to structures ST5 and ST6. These vein systems crosscut the serpentine contact and exhibit subvertical dips of about 80° toward the east. The cobalt arsenide mineralization within these structures displays a characteristic banded texture. Finally, the rose diagram of the mapped fault orientations highlights dominant structural trends, notably N–S and NE–SW (Figure 5b).

4.2.2. Geological mapping underground at a depth of 320 meters (-320)

Figure 6a illustrates the −320 level, which is developed from a main shaft and a network of galleries extending along the contact between serpentinite and diorite, as well as across several transverse veins. These workings clearly expose the contact between serpentinite, gabbroic rocks, and diorite, with an average structural orientation of approximately N125°. The main gallery at this level intersects mineralized veins of various orientations and exhibits variable dip angles. At this level, two main types of mineralized structures have been identified. The first type corresponds to contact-related mineralization occurring along the serpentinite–gabbro or serpentinite–diorite interface, with a dominant WNW–ESE orientation. The second type consists of mineralization hosted within quartz diorite and/or gabbroic mafic rocks, which becomes progressively enriched in cobalt arsenides toward the serpentinite massif. The WNW–ESE-oriented contact-type mineralization is spatially associated with NE-trending left-lateral fault systems. The rose diagram of the mapped fault orientations highlights several dominant structural trends, notably N–S, NE–SW, as well as NW–SE and WNW–ESE (Figure 6b).

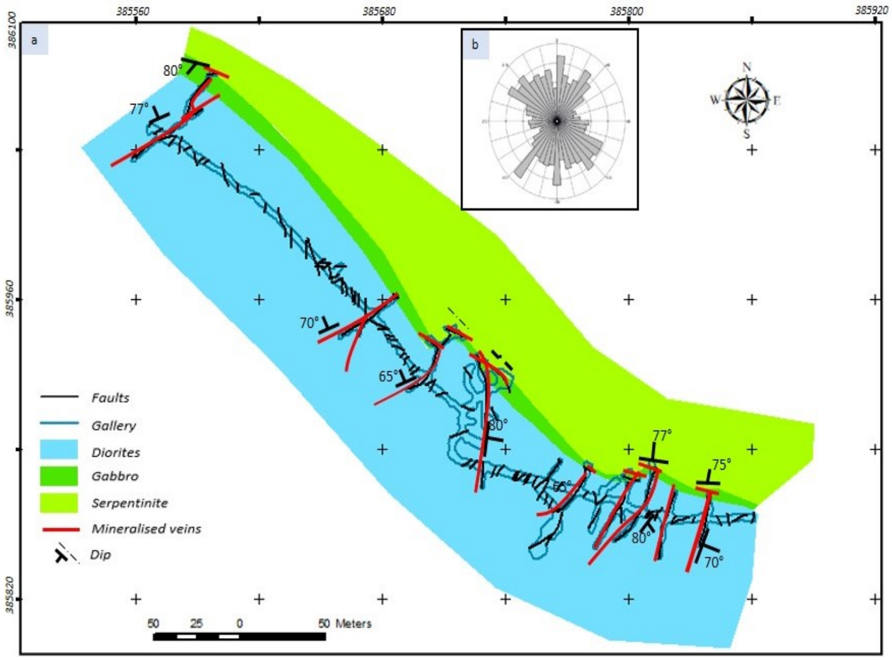

Figure 6. (a) Geological mapping of underground level –320; (b) Rose diagram of lineament orientations

4.3. Structural and mining implications

The results derived from the processing of Landsat 8 OLI satellite data, integrated with detailed underground geological mapping, have enabled the characterization of the structural framework controlling cobalt mineralization within the study area. While several previous studies have primarily focused on the upper levels of the deposits, the present work distinguishes itself by emphasizing the deeper mining levels recently identified, as well as the lateral extensions of the currently exploited zones. In the Aït Ahmane region, cobalt mineralization is spatially associated with a fault network characterized by several dominant orientations, namely WNW–ESE, NE–SW, and N–S. These structures play a key role in governing the localization and distribution of mineralization. In particular, NE-trending left-lateral strike-slip faults have promoted the circulation of mineralizing fluids along contacts between serpentinites and diorites or gabbros.

According to [4], WNW–ESE-oriented faults exhibit a south-verging thrust geometry related to the major Pan-African deformation phase. Furthermore, [41] reported that the emplacement of the Bou Azzer quartz diorite was structurally controlled by left-lateral strike-slip faults oriented between N110° and N120°. This compressional tectonic phase has been attributed by [15] to the late B2 stage of the Pan-African cycle, which affected the upper Cryogenian units of the Bou Azzer Group. Following this compressional regime, the Bou Azzer area underwent an extensional phase contemporaneous with the deposition of the Ouarzazate Group [57,59], characterized by NE–SW-oriented normal faults (N0° to N45°) displaying sinistral kinematics. Finally, a later extensional phase, likely associated with the opening of the Atlantic Ocean at the end of the Triassic, led to the development of ENE–WSW to E–W-oriented normal faults, which dextrally displaced the pre-existing mineralized structures [60].

The cross-analysis of the lineament density map and the geological map reveal a high concentration of lineaments in the southern part of the Aït Ahmane area, particularly within dioritic units, which are characterized by their brittle mechanical behavior. In contrast, the northern sector, dominated by serpentinite massifs and serpentinized basic to ultrabasic rocks, exhibits a lower to negligible lineament density, consistent with the more ductile rheological behavior of these formations [61].

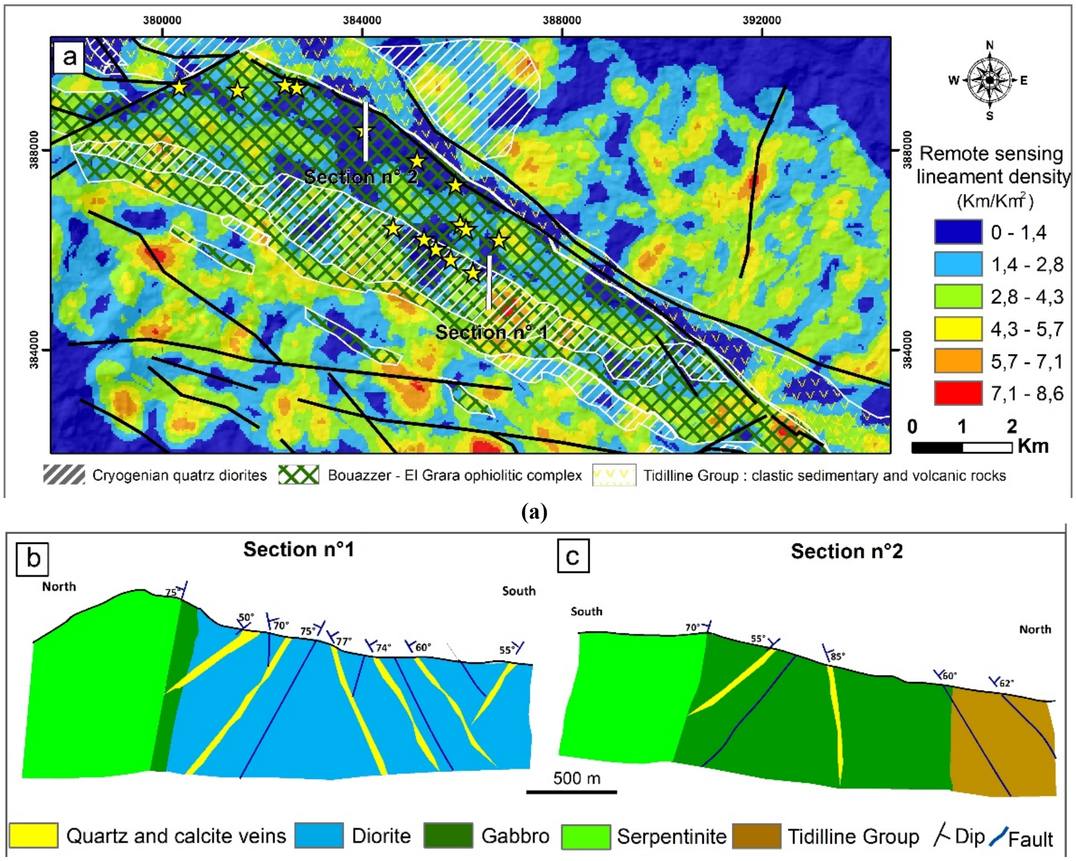

(a)

(b) (c)

Figure 7. (a) Summary of results; (b) synthetic geological cross-section of the northern contact; (c) synthetic geological cross-section of the southern contact

At the northern contact, although fracturing is less intense than at the southern contact, mineral occurrences are commonly observed along the interface between serpentinites, basic rocks, and the volcano-sedimentary formations of the Tiddiline Group (Figure 7c). These mineralized zones are structurally controlled by NE–SW and WNW–ESE-oriented features [6]. To further elucidate the structural controls on cobalt mineralization within the study area, it is essential to emphasize the role of regional fault systems exhibiting various orientations, including WSW–ENE trends, which act as primary metallotectonic controls, as illustrated in Figure 8a. These fault systems inherit the dominant orientation of the main Anti-Atlas Fault, a major regional tectonic structure that has strongly influenced the structural architecture of the area [15].

4.4. Relationship between fracturing, host rock, and mineralization

To validate our results, particularly the contact faults trending WNW–ESE, NW–SE, and NE–SW identified from field geological mapping and Landsat satellite image interpretation, two synthetic geological cross-sections were constructed. These sections were drawn across two key sectors where serpentinite outcrops are particularly well exposed at their contacts with the surrounding host rocks. This approach was supported by detailed field investigations carried out along the two main geological contacts located respectively to the north and south of the serpentinite massif within the study area.

A first structural model is proposed in the form of a NW–SE-oriented geological cross-section established in the field (Figure 7b). This section highlights well-developed vein structures with quartz–carbonate infill hosted within the diorites (Figure 8a, c). These structures, generally oriented N–S to NE–SW, are associated with an extensional tectonic phase responsible for the development of faults oriented between N0° and N40°, crosscutting both diorites and mafic rocks [21]. They display variable dip angles, root at depth, and are predominantly hosted within quartz diorites, which are well recognized as major host rocks for mineralization in the Bou Azzer and Aït Ahmane districts [41].

At the surface, the diorites of the Aït Ahmane area exhibit intense polyphase fracturing, characterized by a dense network of faults and lineaments with multiple orientations (Figure 8b) [18–20]. At depth, within the underground workings of the F53 vein, these extensional structures locally host cobalt mineralization at the contact between serpentinites and gabbroic rocks. Figure 8d illustrates a N10°-oriented structure with a quartz gangue, crosscut by well-developed cobalt arsenide veinlets. This configuration confirms that mafic and ultramafic rocks constitute the principal host lithologies for cobalt mineralization in the study area. In addition, another N–S-oriented structure was identified, crosscutting the diorites and displaying clearly expressed cobalt mineralization (Figure 8e).

In parallel, contact-type cobalt mineralization develops along the interface between serpentinites and gabbros and/or diorites. These structures, oriented WNW–ESE, follow the inherited dip of this geological contact observable at the surface. Such compressive structures played a fundamental role in controlling the localization of mineralization, as suggested by several authors [4,15]. NE–SW-directed compression promoted the development of fluid-draining faults, facilitating the circulation of hydrothermal fluids responsible for mineral deposition along the contacts between serpentinites and mafic rocks or quartz diorites [21]. Figure 8f illustrates a cobalt arsenide–mineralized zone developed along this contact, with an orientation of N120°. The associated carbonation is particularly well developed, as evidenced by underground observations [5,62,63].

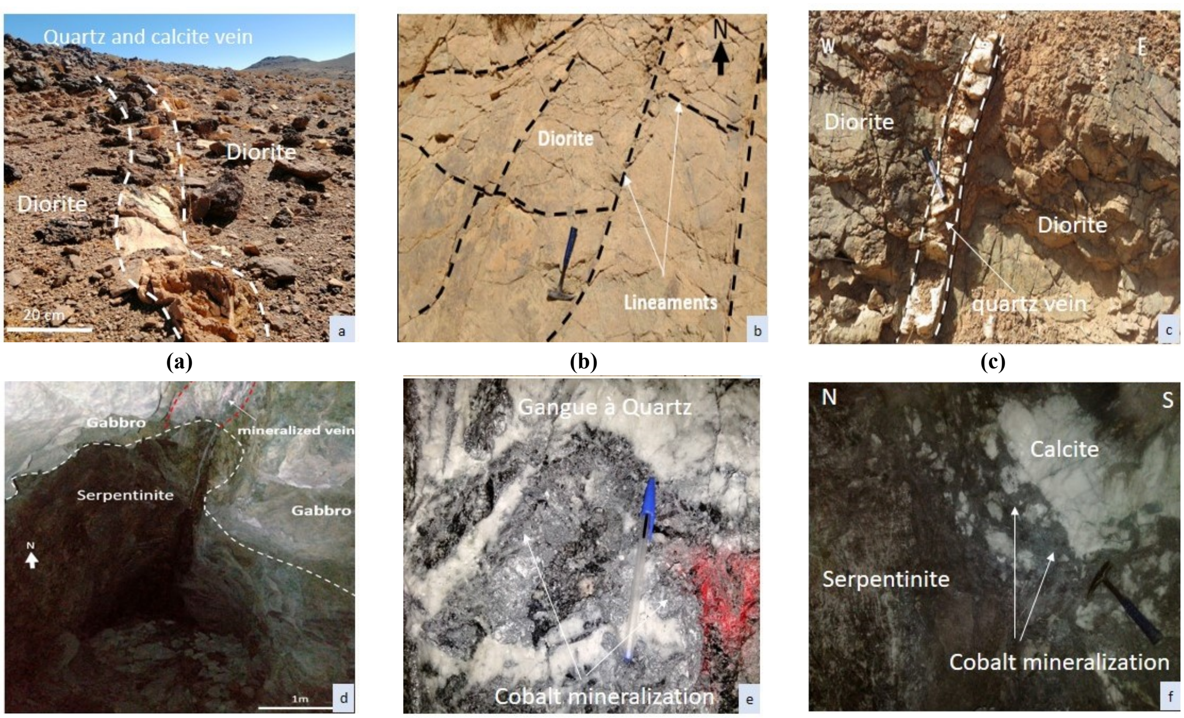

(a) (b) (c) (d) (e) (f)

Figure 8 (a) N–S vein filled with quartz–carbonate; (b) Multidirectional diorite-hosted lineaments; (c) NE–SW quartz vein; (d) N–S vein at the contact between serpentinite and gabbro, with cobaltiferous mineralization; (e) NE–SW intra-diorite vein with cobaltiferous mineralization; (f) WNW–ESE contact mineralization with calcite.

Finally, on the northern flank of the serpentinite massif, a second NE–SW-oriented cross-section (Figure 7c) crossing the F61 deposit, clearly identified on the geological map (Figure 2), highlights a sharp contact between serpentinites and mafic rocks. This compressive contact also favored the concentration of cobalt mineralization in this sector, accompanied by the reactivation of normal faults as both sinistral and dextral strike-slip structures [6]. In this area, well-developed NE–SW-oriented vein structures exhibit subvertical dips and a northward vergence. They are hosted within mafic rocks of microgabbro type, recognized as key host lithologies for cobalt mineralization in the Bou Azzer and Aït Ahmane districts [5,22].

To further validate the results obtained within the study area, a detailed geological survey was conducted along the mining gallery intersecting Structure ST12, located at the northwestern extremity of the lower level of the F54 deposit, along the southern contact (Figure 9a). This structure trends N025° and dips 82° eastward. It is mineralized by cobalt arsenides, represented in this case by skutterudite, which occurs as small cubic crystals visible to the naked eye. The gangue minerals consist mainly of quartz and calcite, forming elongated crystals aligned with the mineralization and displaying a characteristic banded texture (Figure 9b). The quartz diorites are strongly deformed and host significant cobalt mineralization, with Structure ST12 constituting a representative example. Mafic rocks, represented by gabbros, also host cobalt mineralization; however, the thickness and continuity of mineralized zones are comparatively lower than those observed within the diorites. Serpentinites also contain cobalt mineralization at this level, particularly along contacts between carbonated serpentinites and chlorite-rich zones, where calcite patches develop both along the vein walls and within the mineralized zones. This contact trends WNW–ESE and dips approximately 75° southward. Polyphase tectonic deformation is clearly expressed along this gallery, with NE–SW- and N–S-oriented faults affecting both the diorites and the mafic rocks. In addition, the mineralization is offset by E–W-oriented normal faults with dextral displacement and centimetric offsets, indicating that these tectonic structures postdate the mineralization event (Figure 9c). Displacements interpreted as strike-slip offsets affecting the serpentinite contact hosting the cobalt mineralization were also identified. These structures are interpreted as normal–sinistral faults and provide key insights into the structural framework affecting the serpentinite massif, which is considered a primary metallotectonic control for cobalt mineralization. This structural interpretation was developed to guide tactical exploration within the F54 deposit (Figure 9d).

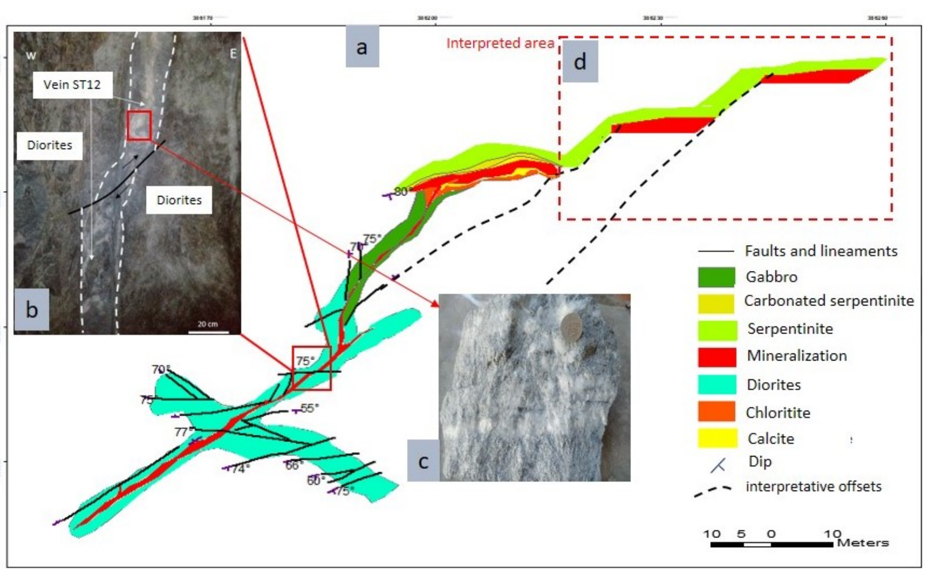

Figure 9. (a) Geological mapping of the ST12 structure at the −320 m level; (b) photograph illustrating the banded texture of the mineralization; (c) photograph of a fault displacing the ST12 mineralized structure; (d) structural interpretation of left-lateral normal (sinistral) strike-slip displacements

4.5. Structural validation Based on Magnetic Lineament Analysis

Figure 10b illustrates the lineaments extracted from the processing of airborne magnetic data using the CET method. These regionally extensive structures show an excellent spatial correspondence with the major tectonic features recognized in the study area.

The CET analysis reveals a dense structural network dominated by preferential orientations N–S, NE–SW, NW–SE, and E–W, in good agreement with results derived from remote sensing and existing geological data.

The identified lineaments closely coincide with major regional faults inherited from the principal Anti-Atlas fault system and play a first-order metallotectonic role. Areas characterized by high CET lineament density (≥ 0.9 km/km²) correspond to the main zones with high potential for cobalt mineralization. These zones reflect a high degree of structural complexity and connectivity, which are favorable for the circulation and concentration of hydrothermal mineralizing fluids. These structures control major lithological contacts between serpentinites and surrounding host rocks, particularly Cryogenian diorites, gabbroic mafic rocks, and Ediacaran volcano-sedimentary formations, which constitute the principal hosts of cobalt mineralization. Notably, the main cobalt deposits and occurrences (F52, F53, F54, F55, F56, F57, F58, F59, F61, and F62) are spatially aligned along these major CET lineaments, especially those associated with the Anti-Atlas fault system. This spatial correlation highlights the fundamental role of these deep-seated structures as deformation corridors and pathways for hydrothermal fluid flow. The alignment of the deposits along CET lineaments therefore confirms a first-order regional structural control on the localization and distribution of cobalt mineralization within the study area.

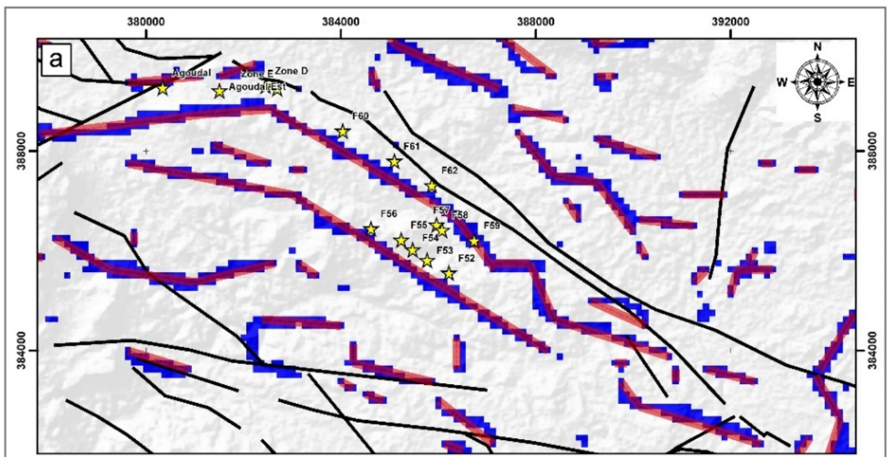

(a)

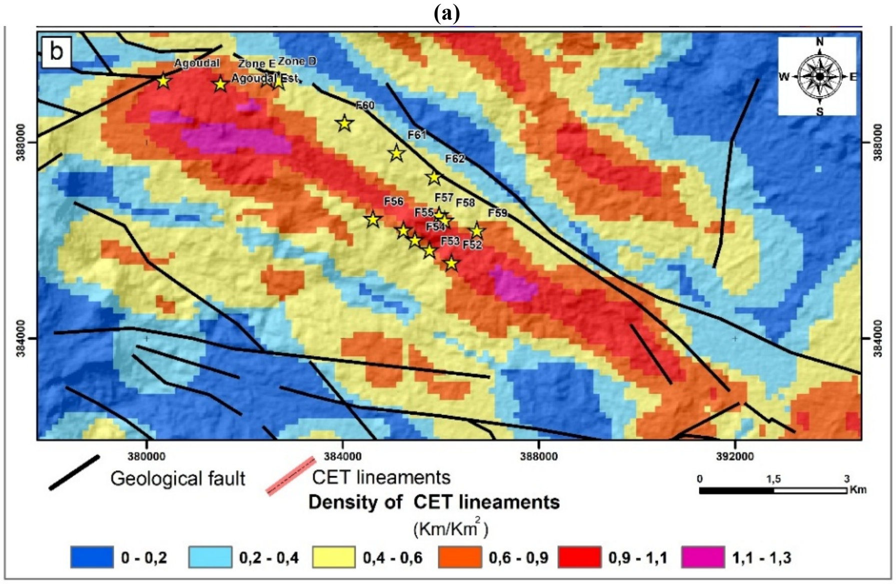

(b)

Figure 10. (a) Spatial correlation between remote sensing–derived lineaments and CET-derived magnetic lineaments; (b) with the associated magnetic lineament density map

5. Conclusions

The present study focuses on the structural mapping analysis of the Ait Ahmane region. The results are derived from the integration of two complementary approaches: multispectral remote sensing, particularly through automated lineament extraction, and geological mapping of subsurface structures. The study area is characterized by a dense fault network, with dominant N–S and NE–SW orientations. These structural trends correspond to mineralization-related structures, including cobalt-bearing veins and associated quartz–carbonate gangue within dioritic intrusions. A secondary set of structures, oriented NW–SE to WNW–ESE, highlights cobalt-mineralized contacts between serpentinites and basic rocks or diorites.

The integration of satellite-derived lineaments with magnetic data and field observations enabled robust validation of the structural framework and provided clearer constraints on the structural control of mineralization.

These results underscore the value of combining remote sensing, magnetic lineament analysis, and detailed geological observations to decipher structural controls and provide a reliable framework for mineral exploration in geologically complex terrains such as the Ait Ahmane area.

References

[1]. Harper, E. M., Kavlak, G., & Graedel, T. E. (2012). Tracking the metal of the goblins: Cobalt's cycle of use. *Environmental Science & Technology, 46*(2), 1079–1086.

[2]. Kissin, S. A. (1992). Five-element (Ni-Co-As-Ag-Bi) veins. *Geoscience Canada, 19*(3). https://journals.lib.unb.ca/index.php/GC/article/view/3768

[3]. Slack, J. F., Kimball, B. E., & Shedd, K. B. (2017). *Critical mineral resources of the United States—Economic and environmental geology and prospects for future supply*. U.S. Geological Survey Professional Paper.

[4]. Admou, H., Philippe, R., Emmanuel, E., Youbi, N., & Soulaimani, A. (2013). *Notice explicative de la Carte géologique du Maroc au 1/50 000, feuille Aït Ahmane*. Notes et Mémoires du Service Géologique du Maroc.

[5]. Bajadi, A., et al. (2024). Assessment of potential cobalt zones by modeling radiometric and ASTER data using the AHP method: A case of the Bou Azzer El Grara inlier, Central Anti-Atlas, Morocco. *Geochemistry, 84*(2), 126105.

[6]. Maacha, L. (2013). *Études métallogéniques et géophysiques des minéralisations cobaltifères et cuprifères de Bou-Azzer El Graara, Anti-Atlas Maroc: Les minéralisations de cuivre de la plateforme de Bleida* [Unpublished doctoral dissertation, Université Cadi Ayyad]. 748 p.

[7]. Sabins, F. F. (1999). Remote sensing for mineral exploration. *Ore Geology Reviews, 14*(3), 157–183.

[8]. Pour, A. B., & Hashim, M. (2012). Identifying areas of high economic-potential copper mineralization using ASTER data in the Urumieh–Dokhtar Volcanic Belt, Iran. *Advances in Space Research, 49*(4), 753–769.

[9]. Rajesh, H. M. (2004). Application of remote sensing and GIS in mineral resource mapping: An overview. *Journal of Mineralogical and Petrological Sciences, 99*(3), 83–103.

[10]. Blein, O., et al. (2014). Geochronological constraints on the polycyclic magmatism in the Bou Azzer-El Graara inlier (Central Anti-Atlas, Morocco). *Journal of African Earth Sciences, 99*, 287–306.

[11]. Bodinier, J. L., Dupuy, C., & Dostal, J. (1984). Geochemistry of Precambrian ophiolites from Bou Azzer, Morocco. *Contributions to Mineralogy and Petrology, 87*(1), 43–50.

[12]. Bouabdellah, M., Maacha, L., Levresse, G., & Saddiqi, O. (2016). The Bou Azzer Co–Ni–Fe–As(±Au ± Ag) district of Central Anti-Atlas, Morocco: A long-lived Late Hercynian to Triassic magmatic-hydrothermal to low-sulphidation epithermal system. In M. Bouabdellah & J. F. Slack (Eds.), *Mineral deposits of North Africa* (pp. 229–247). Springer International Publishing. https://doi.org/10.1007/978-3-319-31733-5_8

[13]. Leblanc, M. (1981). The late Proterozoic ophiolites of Bou Azzer, Morocco: Evidence for Pan-African plate tectonics. In *Developments in Precambrian Geology* (Vol. 4, pp. 435–451). Elsevier.

[14]. Leblanc, M. (1976). Proterozoic oceanic crust at Bou Azzer. *Nature, 261*(5555), 34–35.

[15]. Leblanc, M. (1975). *Ophiolites précambriennes et gîtes arseniés de cobalt: Bou Azzer, Maroc* [Doctoral dissertation, Faculté des Sciences Paris VI]. Mémoires Centre Géologique et Géophysique. https://ci.nii.ac.jp/naid/10018419022/

[16]. Leblanc, M. (1975). Un complexe ophiolitique dans le Précambrien II de l'Anti-Atlas central,

Maroc: Description, interprétation et position stratigraphique. *Notes et Mémoires du Service Géologique du Maroc, 236*, 119–144.

[17]. Ahmadfaraj, M., Mirmohammadi, M., Afzal, P., Yasrebi, A. B., & Carranza, E. J. M. (2019). Fractal modeling and Fry analysis of the relationship between structures and Cu mineralization in Saveh region, Central Iran. *Ore Geology Reviews, 107*, 172–185.

[18]. Ali, M., R, G. M., Peyman, A., & Ali, S. (2021). Fractal modeling and relationship between thrust faults and carbonate-hosted Pb-Zn mineralization in Alborz Mountains, Northern Iran. *Geochemistry, 81*(4).

[19]. Golshan, M. B., Arian, M., Afzal, P., Saein, L. D., & Aleali, M. (2025). Application of fractal models for determining the relationship between REEs and faults in North Kochakali coal deposit, Central Iran. *Scientific Reports, 15*(1), 1276.

[20]. Saadati, H., Afzal, P., Torshizian, H., & Solgi, A. (2025). Application of stepwise fractal modeling for interpretation of remote sensing data, NE Iran. *Iranian Journal of Earth Sciences, 17*(3).

[21]. Ez-Zghoudy, M., et al. (2023). Structural controls on the Co- and Ni-bearing arsenides from the Bou Azzer mine: Case of Aït Ahmane F53 vein deposit: Implications for mineral exploration. *Journal of African Earth Sciences, 202*, 104929.

[22]. Tourneur, E., et al. (2021). Co-Ni-arsenide mineralisation in the Bou Azzer district, Anti-Atlas, Morocco: Genetic model and tectonic implications. *Ore Geology Reviews, 134*, 104128.

[23]. Alaoui, H. E., Moujahid, E., Ibouh, H., Bachnou, A., Babram, M. A., & Harti, A. E. (2016). Mapping and analysis of geological fractures extracted by remote sensing on Landsat TM images: Example of the Imilchil-Tounfite area, Central High Atlas, Morocco. *Estudios Geológicos, 72*(2), 12.

[24]. Javhar, A., et al. (2019). Comparison of multi-resolution optical Landsat-8, Sentinel-2, and radar Sentinel-1 data for automatic lineament extraction: A case study of Alichur area, SE Pamir. *Remote Sensing, 11*(7), 778.

[25]. Ennaciri, A., Barbanson, L., & Touray, J. C. (1995). Mineralized hydrothermal solution cavities in the Co-As Ait Ahmane mine, Bou Azzer, Morocco. *Mineralium Deposita, 30*(1), 75–77.

[26]. Thomas, R. J., et al. (2002). Precambrian evolution of the Sirwa Window, Anti-Atlas Orogen, Morocco. *Precambrian Research, 118*(1), 1–57.

[27]. Bouougri, E. H., et al. (2020). Time constraints on Early Tonian rifting and Cryogenian arc terrane-continent convergence along the northern margin of the West African Craton: Insights from SHRIMP and LA-ICP-MS zircon geochronology in the Pan-African Anti-Atlas belt, Morocco. *Gondwana Research, 85*, 169–188.

[28]. Triantafyllou, A., et al. (2018). Intra-oceanic arc growth driven by magmatic and tectonic processes recorded in the Neoproterozoic Bougmane arc complex, Anti-Atlas, Morocco. *Precambrian Research, 304*, 39–63.

[29]. Ikenne, M., et al. (2021). Cobalt–nickel–copper arsenide, sulfarsenide, and sulfide mineralization in the Bou Azzer window, Anti-Atlas, Morocco: One century of multi-disciplinary and geological investigations, mineral exploration, and mining. *Geological Society, London, Special Publications, 502*(1), 45–66.

[30]. Gasquet, D., Levresse, G., Cheilletz, A., Azizi-Samir, M. R., & Mouttaqi, A. (2005). Contribution to a geodynamic reconstruction of the Anti-Atlas, Morocco, during Pan-African times with emphasis on inversion tectonics and metallogenic activity at the Precambrian–Cambrian transition. *Precambrian Research, 140*(3), 157–182.

[31]. Soulaimani, A., et al. (2013). *Notice explicative de la carte géologique du Maroc au 1/50 000, feuille Al Glo'a.*

[32]. Choubert, G. (1963). *Histoire géologique du Précambrien de l'Anti-Atlas* [Doctoral dissertation]. Notes et Mémoires du Service Géologique du Maroc, 162. 352 p.

[33]. Hefferan, K., et al. (2014). A reconsideration of the Pan-African orogenic cycle in the Anti-Atlas Mountains, Morocco. *Journal of African Earth Sciences, 98*, 34–46.

[34]. Kasten, S., Hefferan, K., & Soulaimani, A. (2017). Anti-Atlas Morocco geochemical and field data analysis indicate Cadomian subduction and collisional tectonism to Ediacaran-Cambrian boundary. *Geological Society of America Abstracts, 49*, 300789.

[35]. Triantafyllou, A., et al. (2016). Neoproterozoic oceanic arc complexes in the Moroccan Anti-Atlas: Tracking their genesis, accretion, and collision. *GB2016*, 226.

[36]. El Hadi, H., et al. (2010). Structural and geochronological constraints on the evolution of the Bou Azzer Neoproterozoic ophiolite, Anti-Atlas, Morocco. *Precambrian Research, 182*(1), 1–14.

[37]. Salmi, S., et al. (2025). Quantification of hydrothermal alteration in Co-Ni-rich mineralized structures along fault segments crossing the Aït Ahmane and Ousdrat plutons, Bou Azzer El-Graara inlier, Central Anti-Atlas: Implications for genesis and mineral exploration. *Journal of Geochemical Exploration, 273*, 107712.

[38]. El Ghorfi, M., et al. (2006). Gold–palladium mineralization at Bleïda Far West, Bou Azzer–El Graara Inlier, Anti-Atlas, Morocco. *Mineralium Deposita, 41*(6), 549–564.

[39]. Maacha, L., et al. (2015). *Arsenide deposits of the Bou Azzer ore district, Anti-Atlas metallogenic province, and their economic outlook*. In V. V. Yarmolyuk (Ed.), *Editor Acad. RAS*.

[40]. Hefferan, K. P., Admou, H., Karson, J. A., & Saquaque, A. (2000). Anti-Atlas, Morocco, role in Neoproterozoic Western Gondwana reconstruction. *Precambrian Research, 103*(1), 89–96.

[41]. Saquaque, A., Admou, H., Karson, J., Hefferan, K., & Reuber, I. (1989). Precambrian accretionary tectonics in the Bou Azzer-El Graara region, Anti-Atlas, Morocco. *Geology, 17*(12), 1107–1110.

[42]. Tourneur, E. (2019). *Circulation de fluides aux abords de failles d'échelle crustale: Contraintes structurales, microtectoniques, inclusions fluides et géochimiques sur les processus de formation du gisement de Bou Azzer (Ni-Co), Anti-Atlas, Maroc* [Doctoral dissertation].

[43]. Goodenough, D. G., et al. (2003). Processing Hyperion and ALI for forest classification. *IEEE Transactions on Geoscience and Remote Sensing, 41*, 1321.

[44]. Adiri, Z., et al. (2017). Comparison of Landsat-8, ASTER, and Sentinel-1 satellite remote sensing data in automatic lineament extraction: A case study of Sidi Flah-Bouskour inlier, Moroccan Anti-Atlas. *Advances in Space Research, 60*(11), 2355–2367.

[45]. Adiri, Z., Harti, A. E., Jellouli, A., Maacha, L., & Bachaoui, E. M. (2016). Lithological mapping using Landsat 8 OLI and Terra ASTER multispectral data in the Bas Drâa inlier, Moroccan Anti-Atlas. *Journal of Applied Remote Sensing, 10*(1), 016005.

[46]. Driouch, A., Ouadif, L., Benjmel, K., Bhilisse, M., & Ilmen, S. (2022). Determining the regional tectonic stress field by remote sensing in the Bou Azzer inlier, Central Anti-Atlas, Morocco. *Mining of Mineral Deposits, 16*(2), 49–54.

[47]. El Janati, M., Soulaimani, A., Admou, H., Youbi, N., Hafid, A., & Hefferan, K. P. (2014). Application of ASTER remote sensing data to geological mapping of basement domains in arid regions: A case study from the Central Anti-Atlas, Iguerda inlier, Morocco. *Arabian Journal of Geosciences, 7*(6), 2407–2422.

[48]. Massironi, M., Bertoldi, L., Calafa, P., Visonà, D., Bistacchi, A., Giardino, C., & Schiavo, A. (2008). Interpretation and processing of ASTER data for geological mapping and granitoids detection in the Saghro Massif, eastern Anti-Atlas, Morocco. *Geosphere, 4*, 736–759.

[49]. Si Mhamdi, H., Raji, M., Maimouni, S., & Oukassou, M. (2017). Fractures network mapping using remote sensing in the Paleozoic massif of Tichka, Western High Atlas, Morocco. *Arabian Journal of Geosciences, 10*(5), 125.

[50]. Si Mhamdi, H., Raji, M., & Oukassou, M. (2016). Utilisation de la télédétection dans la cartographie automatique des linéaments géologiques du granitoïde de Tichka, Haut Atlas Occidental. *European Journal of Scientific Research, 142*, 321–333.

[51]. Anbalagan, R., Kumar, R., Lakshmanan, K., Parida, S., & Neethu, S. (2015). Landslide hazard zonation mapping using frequency ratio and fuzzy logic approach: A case study of Lachung Valley, Sikkim. *Geoenvironmental Disasters, 2*(1), 6.

[52]. Mandal, S., & Maiti, R. (2014). Role of lithological composition and lineaments in landsliding: A case study of Shivkhola watershed, Darjeeling Himalaya. *International Journal of Geology, Earth and Environmental Sciences, 4*, 126–132.

[53]. Matori, A. N., Basith, A., & Harahap, I. S. H. (2012). Study of regional monsoonal effects on landslide hazard zonation in Cameron Highlands, Malaysia. *Arabian Journal of Geosciences, 5*(5), 1069–1084.

[54]. Bajadi, A., et al. (2025). Targeting potential cobalt deposits through integration of helicopter-borne magnetic and stream sediment data: Insights from the Bou Azzer Inlier, Central Anti-Atlas, Morocco. *Ore Geology Reviews, 185*, 106807.

[55]. Holden, E.-J., Wong, J. C., Kovesi, P., Wedge, D., Dentith, M., & Bagas, L. (2012). Identifying structural complexity in aeromagnetic data: An image analysis approach to greenfields gold exploration. *Ore Geology Reviews, 46*, 47–59.

[56]. Kovesi, P. (1997). Symmetry and asymmetry from local phase. In *Tenth Australian Joint Conference on Artificial Intelligence* (pp. 2–4). Citeseer.

[57]. Hinaje, S. (1995). *Apport de l'analyse de la tectonique cassante tardi- et post-panafricaine à la modélisation de la mise en place des minéralisations dans la boutonnière de Bou-Azzer, Anti-Atlas, Maroc*.

[58]. Hung, L. Q., Batelaan, O., & Smedt, F. D. (2005). Lineament extraction and analysis: Comparison of LANDSAT ETM and ASTER imagery. Case study: Suoimuoi tropical karst catchment, Vietnam. In *Remote Sensing for Environmental Monitoring, GIS Applications, and Geology V* (pp. 182–193). SPIE.

[59]. Soulaimani, A., Bouabdelli, M., & Piqué, A. (2003). The Upper Neoproterozoic-Lower Cambrian continental extension in the Anti-Atlas, Morocco. *Bulletin de la Société Géologique de France, 174*(1), 83–92.

[60]. Robert-Charrue, C., & Burkhard, M. (2008). Inversion tectonics, interference pattern, and extensional fault-related folding in the Eastern Anti-Atlas, Morocco. *Swiss Journal of Geosciences, 101*(2), 397–408.

[61]. Bhilisse, M., Admou, H., Aydda, A., & Maacha, L. (2019). Mineralogical and seismic properties of serpentinite of Ait Ahmane fault zone of Bou Azzer ophiolite, central Anti-Atlas of Morocco. *Comptes Rendus Geoscience, 351*(4), 303–311.

[62]. Behbahani, B., Harati, H., Afzal, P., & Lotfi, M. (2023). Determination of alteration zones applying fractal modeling and Spectral Feature Fitting method in Saryazd porphyry copper system, central Iran. *Bulletin of the Mineral Research and Exploration, 2023*(172).

[63]. Saed, S., Azizi, H., Daneshvar, N., Afzal, P., Whattam, S. A., & Mohammad, Y. O. (2022). Hydrothermal alteration mapping using ASTER data, Takab-Baneh area, NW Iran: A key for further exploration of polymetal deposits. *Geocarto International, 37*(26), 11456–11482.

انجمن مهندسی معدن ایران
نشریه مهندسی معدن و محیط زیست
نشانی نشریه: www.jme.shahroodut.ac.ir
دانشگاه صنعتی شاهرود

کنترل ساختاری کانی‌سازی کبالت در منطقه آیت احمانه – بو عزر الغراره اینلیر (آنتی اطلس مرکزی، مراکش): سهم سنجش از دور و نقشه‌برداری زمین‌شناسی زیرزمینی

عبدالحمید بجادی[۱]، دریس العزاب[۱]، انس دریوش[۲]، محمد اوچچن[۳]، و محمد جلال تازی[۱*]

۱. آزمایشگاه تحقیقات علوم و مهندسی، دانشکده علوم و فناوری، دانشگاه سیدی محمد بن عبدالله، فاس، مراکش
۲. آزمایشگاه ژئوفیزیک کاربردی، ژئوتکنیک، زمین شناسی مهندسی و محیط زیست، دانشکده مهندسی محمدیه، دانشگاه محمد پنجم، رباط، مراکش
۳. گروه علوم زمین، دانشکده علوم، دانشگاه ابن زهر، اگادیر، مراکش

اطلاعات مقاله

تاریخ ارسال: ۲۰۲۵/۰۹/۱۶
تاریخ داوری: ۲۰۲۵/۱۲/۳۱
تاریخ پذیرش: ۲۰۲۶/۰۵/۱۰

DOI: 10.22044/jme.2026.16825.3302

کلمات کلیدی

نقشه برداری زمین شناسی زیرزمینی
کنترل ساختاری
کبالت
اکتشاف مواد معدنی

چکیده

درون‌لایه بوازر-الغراره، واقع در آنتی‌اطلس مرکزی مراکش، به دلیل کانی‌سازی قابل توجه کبالت خود که از نظر ژنتیکی با یک توده افیولیتی فوق‌بازی سرپانتینی شده پان‌آفریقایی مرتبط است، شناخته شده است. در این زمینه، یک مطالعه ساختاری در منطقه آیت اهمانه، واقع در انتهای شرقی منطقه معدنی بوازر، با هدف تجزیه و تحلیل خطواره‌های ساختاری، که ابزاری اساسی در نقشه‌برداری زمین‌شناسی و اکتشاف مواد معدنی هستند، انجام شد. رویکرد روش‌شناختی مبتنی بر تفسیر داده‌های سنجش از دور چند طیفی برای نقشه‌برداری خطواره‌های سطحی و مقایسه آنها با ساختارهای مشاهده‌شده در زیر زمین است. پردازش اعمال‌شده بر روی تصاویر OLI لندست ۸ شامل تصحیحات رادیومتری و جوی و به دنبال آن تجزیه و تحلیل مؤلفه‌های اصلی (PCA) است که تمایز ساختارهای خطی را افزایش می‌دهد و امکان تولید نقشه‌های خطواره‌ای قابل اعتماد را فراهم می‌کند. به طور موازی، نقشه‌برداری زمین‌شناسی زیرزمینی در کانسار رگه‌ای F53، در دو سطح بهره‌برداری پایین‌تر، برای توصیف ساختارهای معدنی در عمق انجام شد. ادغام مجموعه داده‌های سطحی و زیرسطحی، دو خانواده ساختاری اصلی را برجسته می‌کند. اولی، با روند N-S تا NE-SW، با ساختارهای حاوی کبالت که در دیوریت‌ها قرار دارند مرتبط است. دومی، با جهت‌گیری NW-SE تا WNW-ESE، مربوط به تماس‌های تکتونولی-لیتولوژیکی کانی‌سازی شده با کبالت بین سرپانتینیت‌ها، سنگ‌های بازیک و دیوریت‌ها است. همبستگی بین خطواره‌های نقشه‌برداری شده سطحی و ساختارهای عمیق قابل توجه است و بر پیوستگی ساختاری بین حوزه‌های سطحی و زیرسطحی تأکید می‌کند.

نویسنده مسئول مکاتبات: *mohammedjalaltazi.tazi@usmba.ac.ma* (م.ج. تازی)